IEEE Robotics and Automation Letters (RAL) paper presented at the
2020 IEEE/RSJ International Conference on Intelligent Robots and Systems (IROS)
October 25-29, 2020, Las Vegas, NV, USA (Virtual)

Enhancement of Force Exertion Capability of a Mobile Manipulator by Kinematic Reconfiguration

Hongjun Xing[1,2], Ali Torabi[2], Liang Ding[1*], *Senior Member, IEEE*, Haibo Gao[1], Zongquan Deng[1], and Mahdi Tavakoli[2*], *Senior Member, IEEE*

***Abstract*— With the increasing applications of wheeled mobile manipulators (WMMs), new challenges have arisen in terms of executing high-force tasks while maintaining precise trajectory tracking. A WMM, which consists of a manipulator mounted on a mobile base, is often a kinematically redundant robot. The existing WMM configuration optimization methods for redundant WMMs are conducted in the null-space of the entire system. Such methods do not consider the differences between the mobile base and the manipulator, such as their different kinematics, dynamics, or operating conditions. This may inevitably reduce the force exertion capability and degrade the tracking precision of the WMM. To enhance the force exertion capability of a WMM, this paper maximizes the directional manipulability (DM) of the manipulator, with consideration of the joint torque differences, first in Cartesian space and then in the null-space of the robotic system. To maintain precise end-effector trajectory tracking, this paper proposes a novel coordination method between the mobile base and the manipulator via a weighting matrix. The advantages and effectiveness of the proposed approach are demonstrated through experiments.**

I. Introduction

Due to their great mobility and desirable operation capability, wheeled mobile manipulators (WMMs) have been widely employed in many applications, including logistics, disaster rescue, and home/service applications [1], [2]. The integration of a mobile base with a standard manipulator can greatly enlarge its workspace and provide it with more degrees of freedom (DOFs). However, this combination will also bring new challenges. First, the models and operating conditions (i.e., interacting environments) for the mobile base and the manipulator are different; the base usually moves in an unstructured environment with complex dynamics and the manipulator is often in free/contact motion [3]. Second, a WMM is often a kinematically redundant robotic system due to the mix of the mobile base and the manipulator – a redundant robot has more DOFs than minimally required for performing tasks. How to use the redundancy of the WMM to execute sub-tasks (i.e., secondary goals besides the primary goal, which is typically trajectory tracking) remains an interesting research field.

Kinematic modelling and motion control for WMMs have been conducted in many studies following two fundamental approaches. Some authors add the mobile base-imposed constraints directly to the manipulator model [4], which focuses on methods to decouple the control of the two subsystems but cannot control the entire WMM system via one controller. Others explicitly formulate the admissible motions with respect to the base constraints [5], which consider the WMM as one system with a dynamic effect between the base and the manipulator taken into account. The latter approach is adopted in this work because the tasks in this paper require that the manipulator and the base operate simultaneously.

The entire model for the WMM is usually redundant for a given task, which means there are more DOFs in the system than the task needs. Many redundancy resolution methods for standard redundant manipulators can be extended to WMMs including the reduced gradient-based method [6], the damped least-squares inverse Jacobian method [7], and the weighted inverse Jacobian method [8]. Furthermore, the self-motion of the WMM can be used to execute sub-tasks, such as joint limit and obstacle avoidance, manipulability maximization, or singularity avoidance [3], [9], [10].

Most of the previous work views the mobile base as a new addition to the manipulator without considering the inherent differences in the dynamics and working environments between them. This approach results in considerable tracking errors for the end-effector motion due to the typically low positioning precision of the mobile base [11]. For kinematic control, Jia *et al.* [12] addressed this discrepancy between the mobile base and the manipulator and proposed a coordinated motion control method based on adaptive motion distribution for nonholonomic mobile manipulator without considering the joint limits (position, velocity, and acceleration). For dynamic control, many other dynamic control techniques can be employed including neural networks, adaptive control [13], [14].

Besides trajectory following, a WMM can be employed in payload handling tasks where it has to apply large forces to

This work was supported by Canada Foundation for Innovation (CFI), the Natural Sciences and Engineering Research Council (NSERC) of Canada, the Canadian Institutes of Health Research (CIHR), the Alberta Advanced Education Ministry, the Alberta Economic Development, Trade and Tourism Ministry's grant to Centre for Autonomous Systems in Strengthening Future Communities, the National Natural Science Foundation of China (Grant No. 51822502, 91948202), the National Key Research and Development Program of China (No. SQ2019YFB130016), the Fundamental Research Funds for the Central Universities (Grant No. HIT.BRETIV201903), the "111" Project (Grant No. B07018), and the China Scholarship Council under Grant [2019]110. (Liang Ding and Mahdi Tavakoli are the corresponding authors).

[1]H. Xing, L. Ding, H. Gao, and Z. Deng are with the State Key Laboratory of Robotics and System, Harbin Institute of Technology, Harbin 150001, China. {xinghj, liangding, gaohaibo, dengzq}@hit.edu.cn

[2]H. Xing, A. Torabi, and M. Tavakoli are with the Department of Electrical and Computer Engineering, University of Alberta, Edmonton T6G 1H9, Alberta, Canada. {xhongjun, ali.torabi, mahdi.tavakoli}@ualberta.ca

its environment. In these cases, for enhancing the force exertion capability, the redundancy of the WMM can be utilized via its null-space by defining a proper objective (i.e., the subtask). Force manipulability ellipsoid, proposed by Yoshikawa [10], is a useful tool for visualizing the force transmission characteristics of a robot at a given configuration [15]. Later, this measure has been extended to mobile manipulators [9]. The force manipulability ellipsoid is a measure showing the force exertion capability of a robot in all directions in the Cartesian space, and it can be enlarged using a null-space controller for the redundant robot [9]. Chiu [16] proposed the concept of task compatibility, which can optimize the velocity or force requirements in a given direction. With the consideration of joint torque differences, Ajoudani *et al.* [17] improved this concept by introducing a weighting matrix to scale the joint torques. However, all these objectives were optimized only in the null-space.

In the literature, the studies about improving the trajectory tracking precision have been conducted mostly in the context of dynamic control of WMMs where complicated control strategies have been used yet the system's stability is usually hard to be guaranteed [18]. In the context of kinematic control, the coordinated control of a WMM usually ignores the difference in the motion tracking accuracies achievable by the mobile base versus the manipulator [19], and the manipulator's joint limits (position, velocity, and acceleration) are usually not considered [12]. For enhancing the manipulability, most of the recent work only considers the null-space optimization, without considering any optimization in Cartesian space for better manipulability [20].

The main contribution of this paper is to propose a method to enhance the force exertion capability of a WMM in any given direction while trying the best to pursue the tracking precision of the end-effector. With this novel approach, these two goals can be achieved by first employing a weighting matrix to decompose the total desired motion for the WMM to a motion for the mobile base and another motion for the manipulator. Second, we enhance the "directional manipulability" (DM) of the manipulator in both the Cartesian space and the null-space, which is defined with consideration of joint torque differences. It should be emphasized that it is a trade-off between acquiring high tracking accuracy and achieving desirable force exertion capability.

In terms of the primary goal of trajectory tracking, the manipulator's joint limits are taken into account and, where possible, it is tried to employ only the manipulator joints due to the slippage and modelling errors of the mobile base. When the desired end-effector trajectory is beyond the workspace of the manipulator, however, the controller will transfer some of the total motion requirements to the mobile base. In terms of the secondary goal of maximizing the force exertion capability, the first step to improve the DM is by adjusting the end-effector position via Cartesian space control, and then by using the self-motion via null-space control.

The remainder of this paper is organized as follows. In Section II, the kinematic model for a WMM is provided. In Section III, kinematic control of the WMM with consideration of DM enhancement and trajectory tracking is presented. Experiments that demonstrate the validity and performance of the proposed method are presented in Section IV. Section V concludes the manuscript.

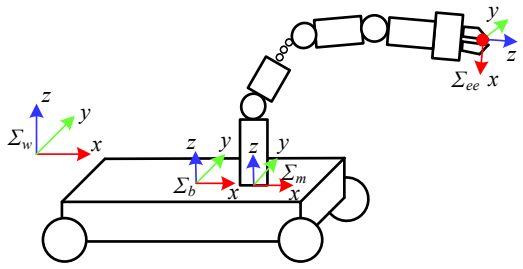

Fig. 1: Kinematic model representation of the mobile manipulator.

II. Kinematic Modeling of Wheeled Mobile Manipulators

In order to plan the motion of the end-effector of a wheeled mobile manipulator, the kinematics for the mobile manipulator should be established. The kinematic modelling contains two parts: the first is the forward kinematics, which given the joint positions calculates the robot's end-effector pose (position and orientation) and the second is the inverse kinematics that given the end-effector pose leads to the joint positions. For a redundant robot, the latter is usually an optimization process in which the redundancy of the robot is utilized in different ways to realize different sub-tasks in parallel to the main task [21].

The forward kinematics for a mobile manipulator can be derived from the kinematic models of the two subsystems, i.e., the mobile base and the manipulator. Fig. 1 shows a standard WMM with reference coordinates defined. We denote Σ_w, Σ_b, Σ_m, and Σ_{ee} as the world reference frame, mobile base frame, manipulator reference frame, and end-effector frame, respectively. The forward kinematics of the manipulator with respect to Σ_m can be expressed as

$$x_m = h_m(q_m), \tag{1}$$

where $x_m \in \mathbb{R}^r$ is the pose of the end-effector in Σ_m, $h_m(q_m)$ denotes the forward kinematics for the manipulator, and $q_m \in \mathbb{R}^m$ is the generalized manipulator coordinate. Then, the forward kinematics for the entire WMM can be expressed as

$$x(q) = x_w(q) = h(q_b, q_m) = Tq_b + T_b^w(q_b)T_m^b h_m(q_m), \tag{2}$$

where $x \in \mathbb{R}^r$ is the pose of the end-effector in Σ_w; $q = [q_b^{\mathrm{T}}, q_m^{\mathrm{T}}]^{\mathrm{T}} \in \mathbb{R}^n$, $q_b \in \mathbb{R}^{n_b}$ are the generalized coordinates for the WMM and the mobile base, respectively; $T \in \mathbb{R}^{r \times n_b}$ is a constant transformation matrix, which expresses the relationship between the coordinates of the mobile base and the pose of the end-effector; $T_b^w(q_b) \in \mathbb{R}^{r \times r}$ is the

transformation matrix from Σ_b to Σ_w; and $T_m^b \in \mathbb{R}^{r\times r}$ is a constant matrix to express the origin of Σ_m in Σ_b.

Assuming a pure rolling contact between the wheels of the mobile base and the ground (i.e., no slippage), the mobile base kinematic model can be derived as

$$\dot{q}_b = P(q_b)v_b, \tag{3}$$

where $v_b \in \mathbb{R}^b$ is the velocity of the wheels, and $P(q_b) \in \mathbb{R}^{n_b\times b}$ is the constraint matrix of the base (holonomic or nonholonomic), which transfers the wheel velocities to the generalized base velocities. The model for slippery wheels can be found in other literature from our group [22] but we will not consider wheel slippage in this work. The generalized velocities for the manipulator can be expressed using the joint velocities as

$$\dot{q}_m = v_m, \tag{4}$$

where $v_m \in \mathbb{R}^m$ is the velocity of the manipulator joints.

The complete velocity input vector for the WMM can be expressed as $v = [v_b^{\mathrm{T}}, v_m^{\mathrm{T}}]^{\mathrm{T}} \in \mathbb{R}^{b+m}$. The end-effector velocity is actually the differential of (2) with respect to time. Combining (3) and (4) yields

$$\begin{aligned}\dot{x} = J_q(q)\dot{q} &= [J_b(q) \quad J_m(q)]\begin{bmatrix}\dot{q}_b\\ \dot{q}_m\end{bmatrix}\\ &= [J_b(q) \quad J_m(q)]\begin{bmatrix}P(q_b)v_b\\ v_m\end{bmatrix}\\ &= [J_b(q)P(q_b) \quad J_m(q)]\begin{bmatrix}v_b\\ v_m\end{bmatrix} = J(q)v,\end{aligned} \tag{5}$$

where $J_b(q) \in \mathbb{R}^{r\times n_b}$ is the Jacobian of the mobile base, $J_m(q) \in \mathbb{R}^{r\times m}$ is the Jacobian of the manipulator, $J_q(q) \in \mathbb{R}^{r\times n}$ is the Jacobian of the unconstrained WMM, and $J(q) \in \mathbb{R}^{r\times(b+m)}$ is the Jacobian of the WMM. It is worth noting that there are two Jacobians for a WMM just because the generalized velocity $\dot{q}_b$ for the mobile base is not its wheel velocity v_b.

The inverse kinematics of the WMM can be built by resorting to an optimization technique that solves the set of generalized coordinates given an end-effector desired pose. The cost function for the WMM can be written as

$$\begin{aligned}&\min_{\dot{q}} H(\dot{q}) = \frac{1}{2}(\dot{q}-\dot{q}_0)^{\mathrm{T}}Q(\dot{q}-\dot{q}_0),\\ &\text{s.t.} \qquad \dot{x} = J_q(q)\dot{q},\end{aligned} \tag{6}$$

where $Q \in \mathbb{R}^{n\times n}$ is a symmetric and positive definite weighting matrix, $\dot{q}_0 \in \mathbb{R}^n$ is the desired value for the joint velocity, and $J_q(q) \in \mathbb{R}^{r\times n}$ is the robot Jacobian as shown in (5). Then, we can obtain the solution to the optimization problem in (6) as (for brevity the dependence of the variables upon the joint variables are omitted)

$$\dot{q} = J_q^{\dagger}\dot{x} + (I_{n\times n} - J_q^{\dagger}J_q)\dot{q}_0, \tag{7}$$

where $J_q^{\dagger} = Q^{-1}J_q^{\mathrm{T}}(J_qQ^{-1}J_q^{\mathrm{T}})^{-1}$ is the weighted pseudoinverse of J_q, and $I_{n\times n}$ is an $n\times n$ identity matrix. The method to choose Q will be discussed in Section III-B.

III. Kinematic Control of Mobile Manipulators with Directional Manipulability Enhancement

A. Directional Manipulability

Mobile manipulation can realize mobility and manipulability simultaneously, and for a redundant robot, the redundancy can be used to execute sub-tasks via the null-space controller. As shown in (7), the different choice of $\dot{q}_0 = \nabla_q H(q)$ can achieve different objectives without affecting the main task $\dot{x}$, since all the motion of $\dot{q}_0$ is projected in the null-space of J_q, and $H(q)$ is the differentiable objective function. It should be noted that the optimization in this paper is focused on the manipulator since the mobile base is mainly used to enhance the mobility of the system.

Yoshikawa first provided manipulability index for velocity manipulability ellipsoid as a design quality measure [10] defined as $H_1(q_m) = \sqrt{\det[J_mJ_m^{\mathrm{T}}]}$. The maximization of H_1 can simultaneously maximize the "distance" of the manipulator from singularities and let the manipulator use the least joint velocities to generate the same end-effector velocities (inclusion of translational and angular velocities). However, the focus of this paper is on force exertion capability similar to the definition of force manipulability ellipsoid. It is essential to note that the force manipulability ellipsoid is the inverse of the velocity manipulability ellipsoid. This means that the direction along which the manipulator has the largest force/torque capability is perpendicular to the direction along which the manipulator uses the least joint velocities. This is a very important optimization objective, especially when the manipulator moves in contact environment. For a specific task, however, it is not necessary to pursue the maximum force manipulability for every direction. It is just a waste of optimization ability. Instead, the force manipulability should be enhanced in a needed direction for the best results. Also, the torque limit differences of the joints are not considered in force manipulability, which is a disadvantage of this measure. If a specific optimization direction for the end-effector in the world frame, say $u \in \mathbb{R}^r$, is given, with the consideration of the joint torque limits of the manipulator, the directional manipulability can be defined as [17]

$$H_2(q) = [u^{\mathrm{T}}(J_mW_\tau^{\mathrm{T}}W_\tau J_m^{\mathrm{T}})u]^{-1/2}, \tag{8}$$

where $W_\tau = \mathrm{diag}[\frac{1}{\tau_{\mathrm{lim}_1}} \ \frac{1}{\tau_{\mathrm{lim}_2}} \ \cdots \ \frac{1}{\tau_{\mathrm{lim}_m}}]$ is a scaling matrix to normalize the joint torques, and τ_{lim_i} represents the torque limit of the i^{th} joint.

In the literature, the manipulability measure H_1 has been maximized in the null-space of WMM to improve its manipulability and avoid the singularity. To best of our knowledge, the optimization of DM has never been done for a WMM in the literature (not even in its null-space). In this research, however, we enhance the DM H_2 in both Cartesian space and null-space for force exertion capability enhancement of the mobile manipulators. As shown in (8), if the direction u is assumed to have no relation with the generalized coordinates of the manipulator q_m, then the partial derivative of H_2 to

$q_{m,i}$ can be calculated as

$$\begin{aligned}\nabla_{q_{m,i}} H_2 &= \frac{-H_2^{-\frac{3}{2}}}{2} \frac{\partial (u^{\mathrm{T}} J_m W_\tau^{\mathrm{T}} W_\tau J_m^{\mathrm{T}} u)}{\partial q_{m,i}} \\ &= \frac{-u^{\mathrm{T}} H_2^{-\frac{3}{2}}}{2} \frac{\partial (J_m W_\tau^{\mathrm{T}} W_\tau J_m^{\mathrm{T}})}{\partial q_{m,i}} u,\end{aligned} \tag{9}$$

where $q_{m,i}$ is the i^{th} joint coordinate and $\nabla_{q_m} H_2 = [\nabla_{q_{m,1}} H_2 \ \nabla_{q_{m,2}} H_2 \ \cdots \ \nabla_{q_{m,m}} H_2]$.

For optimization in the Cartesian space, the partial derivative of H_2 to x_i can be expressed as

$$\nabla_{x_i} H_2 = \frac{\partial H_2}{\partial q_m} \frac{\partial q_m}{\partial x_i} = \nabla_{q_{m,i}} H_2 \ J_{m,i}^{\dagger}, \tag{10}$$

where x_i is the i^{th} component of the end-effector pose and $\nabla_x H_2 = [\nabla_{x_1} H_2 \ \nabla_{x_2} H_2 \ \cdots \ \nabla_{x_r} H_2]$, and it should be emphasized that the optimization on the Cartesian space and the null-space cannot be conducted simultaneously to avoid instability of the robotic system.

It is worth mentioning that by enhancing DM of the manipulator in a given direction, the manipulator will only change to a configuration close to singularity (not reach singularity) to derive the optimal force exertion capability. If the manipulator is too close to singularity to make the system unstable, then, the user can avoid this by using damped least-squares method [23]. A criterion to detect whether the manipulator is close to singularity is defined based on the minimum singular value of the Jacobian matrix [24]. When the minimum singular value is below a predefined threshold, the weighted pseudoinverse method will be changed into damped least-squares method to avoid introducing instability to the robotic system. However, this operation may reduce the maximal force exertion capability of the system.

B. Weighting Matrix Adjustment

The weighting matrix in (7) plays an essential role in splitting the joint motion for the WMM when the desired end-effector Cartesian movement is determined. For a WMM, the properties for the mobile base and the manipulator, such as mass and inertia, are different and the working conditions for them are not the same either. Usually, the positioning precision of the mobile base is worse than that of the manipulator and, thus, it is desirable to command more joint motion to the manipulator of the WMM.

The weighting matrix Q in (7) is replaced by defining a new variable $W_x = Q^{-1}$ in the following sections for better expression. Also, instead of using the unconstrained Jacobian J_q in (7), we choose the entire system Jacobian J in (5) to command motion to each actuator of the WMM. The weighted pseudoinverse of J is expressed as

$$J^{\dagger} = W_x J^{\mathrm{T}} (J W_x J^{\mathrm{T}})^{-1} \tag{11}$$

with the weighting matrix $W_x \in \mathbb{R}^{(b+m)\times(b+m)}$ defined as

$$W_x = \begin{bmatrix} \gamma I_{b\times b} & 0_{b\times m} \\ 0_{n_m\times b} & (1-\gamma) I_{m\times m} \end{bmatrix}, \tag{12}$$

where $\gamma \in [0,1]$ is the parameter determining the motion weighting between the mobile base and the manipulator. $\gamma = 0$ means that the entire end-effector motion depends on the manipulator, $\gamma = 1$ means that the motion is realized solely by the mobile base, and $\gamma \in (0,1)$ means that the end-effector motion is achieved via both the manipulator and the mobile base.

To further demonstrate this method, consider a simple 3-DOF serial manipulator with joint coordinate vector denoted as $q = [q_1, q_2, q_3]^{\mathrm{T}}$, if the additional joint motion requirement besides the trajectory tracking task is expressed as $q_1 = 2q_2 = 4q_3$, then, the corresponding weighting matrix for this system can be defined as $W_x = \mathrm{diag}[1, 1/2, 1/4]$, which may not achieve the desired joint motion trajectory (due to the Cartesian space trajectory), but can obtain a desirable one.

When the range or velocity requirement of the task exceeds the limit of the manipulator, the mobile base should be involved. Assuming that the WMM is controlled at the velocity level, the constraints on joint velocity are locally calculated taking into account the joint range, velocity and acceleration bounds of the manipulator. The motion limit of the manipulator's joints can be expressed at the current configuration as [25]

$$\dot{Q}_{\min}(q_m) \leqslant \dot{q}_m \leqslant \dot{Q}_{\max}(q_m), \tag{13}$$

where $\dot{Q}_{\max}(q_m)$ and $\dot{Q}_{\min}(q_m)$ are the upper and lower joint velocity limits of the manipulator, respectively. If the velocity command of the manipulator joints $\dot{q}_m$ exceeds the velocity limit defined in (13), which means that the sole manipulator motion cannot cover the end-effector motion requirement, then γ should be increased to split more motions to the base.

The parameter γ can be adjusted as

$$\gamma = \begin{cases} 0 & \text{if } \eta \leqslant \epsilon \\ \eta & \text{if } \epsilon < \eta \leqslant 1 \\ 1 & \text{if } \eta > 1, \end{cases} \tag{14}$$

where ϵ is the upper limit of the motion distribution without mobile base, which will be determined by the user through trial and error, and $\eta = \max\left\{ \frac{|\dot{q}_{m,i}|}{|\dot{Q}_{\max,i}|}, \frac{|\dot{q}_{m,i}|}{|\dot{Q}_{\min,i}|} \right\}$ with $i = 1, 2, \cdots, m$. A similar method has also been adopted in [12].

When the manipulator is within its admissible velocity limits, $\gamma = 0$ to transfer no motion to the mobile base. If the manipulator approaches its velocity limit, the manipulator cannot handle the task alone, and γ will be set equal to η to let the mobile base share part of the motion. Finally, when the manipulator command exceeds its velocity limit, γ will be set equal to one to let the mobile base solely undertake the motion requirement.

C. Kinematic Control of Mobile Manipulators

As stated before, the target of this paper is threefold: first to complete trajectory tracking by using WMM, second to optimize DM of the manipulator to make it stay in optimal configuration for exerting large forces, and third to transfer motion requirement to the manipulator as far as possible in

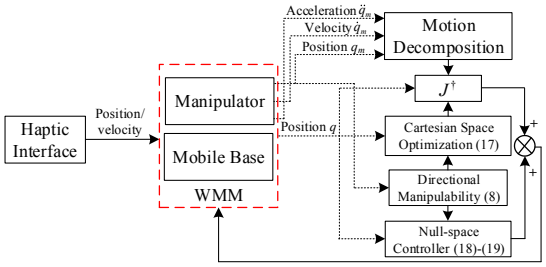

Fig. 2: Block diagram of the control system.

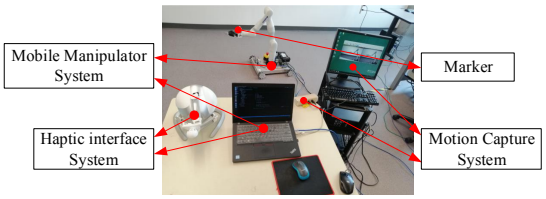

Fig. 3: Experimental setup.

order to have the best motion precision (remembering that mobile bases often have inferior positioning accuracies).

According to (5) and (7), the entire kinematic controller of the WMM can be designed as

$$v = J^\dagger \dot{x} + (I_{(b+m)\times(b+m)} - J^\dagger J) v_0, \tag{15}$$

where $J^\dagger$ is the weighted pseudoinverse of J with the definition in (11)-(12), and $v_0 \in \mathbb{R}^{b+m}$ is the self-motion velocity for sub-tasks in the null-space.

For DM enhancement in Cartesian space, the null-space controller can be omitted, and controller (15) is rewritten as

$$v = J^\dagger v_c \tag{16}$$

with $v_{c,i}$ defined as

$$v_{c,i} = \begin{cases} k_C \left[(\nabla_x H_2)^{\mathrm{T}} \right]_i & \text{if } x_{\min,i} \leqslant x_i \leqslant x_{\max,i} \\ 0 & \text{else}, \end{cases} \tag{17}$$

where $i = 1, 2, \cdots, r$, $v_{c,i}$ is the i^{th} component of v_c, k_C is a positive scalar gain, and $x_{\max,i}$ and $x_{\min,i}$ are the upper and lower limits of the i^{th} component of the permissible position for the end-effector, respectively.

For DM enhancement in null-space of the WMM, the controller (15) can be designed as

$$v = J^\dagger (\dot{x}_d + K_x (x_d - x)) + (I_{(b+m)\times(b+m)} - J^\dagger J) v_n. \tag{18}$$

Here, $x \in \mathbb{R}^r$ and $x_d \in \mathbb{R}^r$ are the actual and desired poses of the end-effector, respectively, $K_x \in \mathbb{R}^{r\times r}$ is a constant gain matrix, and v_n is defined as

$$v_n = k_N \begin{bmatrix} 0_{b\times 1} \\ (\nabla_{q_m} H_2)^{\mathrm{T}} \end{bmatrix}, \tag{19}$$

where k_N is a positive scalar gain. The desired end-effector trajectory $\dot{x}$ in (15) is changed to $\dot{x}_d + K_x(x_d - x)$ in (18) to make sure the trajectory tracking error convergences to zero. Accurate end-effector trajectory tracking is realized by adjusting the weighting matrix designed in Section III-B. A block diagram of the control system is shown in Fig. 2, where the haptic interface will provide the motion command for the WMM system when needed.

IV. Experimental Results

Several experiments have been conducted to verify the effectiveness of the proposed kinematic control method for WMMs. The experiments in this section contain two parts: (A) the verification of the weighting matrix adjustment method to improve tracking accuracy, and (B) the evaluation of the DM enhancement to increase force exertion capability.

A. Experimental Setup

In this study, we use an omnidirectional wheeled mobile manipulator, which is composed of a custom-built four-wheel mobile base and a 7-DOF ultra-lightweight robotic arm Kinova Gen3 (Kinova Robotics, Canada), and the mobile base frame Σ_b coincides with the manipulator reference frame Σ_m. The mobile base is equipped with two pairs of Mecanum wheels so that it can realize omnidirectional motion, which shortens robot throughput times and reduces nonproductive time when searching appropriate execution pose for a given task [26].

The experimental setup is shown in Fig. 3. It consists of a 4-wheel omnidirectional mobile manipulator as the slave robot, a Falcon haptic interface (Novint Technologies Inc., USA) as the master robot, and a motion capture system (Claron Technology Inc., Canada). The haptic interface is used to send position/velocity commands to the WMM, and the motion capture system is employed to evaluate the tracking accuracy of the end-effector and not used in the control system.

The mobile base has less motion precision compared with the manipulator due to uncertain wheel-ground contact or wheel wear [12]. It should be noted that the manipulator is installed on the mobile base, so even small motion errors of the base, in particular the turning errors, will result in large position errors of the end-effector.

The joint velocity limit of the manipulator is expressed for motion decomposition as (13). The generalized coordinates for the mobile base (shown in Fig. 4) are defined as $q_b = [x_b, y_b, \theta_b]^{\mathrm{T}} \in \mathbb{R}^3$ and the velocity command of the wheels as $v_b = [\omega_1, \omega_2, \omega_3, \omega_4]^{\mathrm{T}} \in \mathbb{R}^4$. The velocity transformation matrix $P(q_b) \in \mathbb{R}^{3\times 4}$, which transfers the wheel velocities to the generalized base velocities, can be expressed as

$$P(q_b) = J_I J_V \tag{20}$$

with $J_I = \begin{bmatrix} \cos\theta_b & -\sin\theta_b & 0 \\ \sin\theta_b & \cos\theta_b & 0 \\ 0 & 0 & 1 \end{bmatrix}$, and $J_V = \frac{R}{4} \begin{bmatrix} 1 & 1 & 1 & 1 \\ -1 & 1 & 1 & -1 \\ \frac{-1}{l_1+l_2} & \frac{1}{l_1+l_2} & \frac{-1}{l_1+l_2} & \frac{1}{l_1+l_2} \end{bmatrix}$. The variables θ_b, R, l_1, and l_2 are illustrated in Fig. 4.

In this research, no constraint is imposed on the orientation of the end-effector of the WMM. Therefore, the

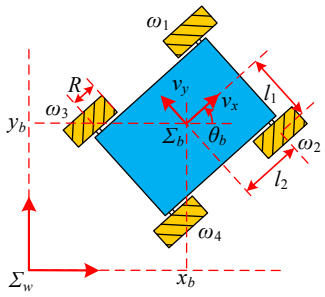

Fig. 4: Kinematics of the omnidirectional mobile base.

TABLE I: Maximum and RMS values of commanded base velocity using two kinematic control methods

	v_{xb} (cm/s)		v_{yb} (cm/s)		ω_b (°/s)	
	Max.	RMS	Max.	RMS	Max.	RMS
Proposed	2.8	1.68	1.72	0.65	0.0917	0.035
Traditional	3.91	2.58	2.38	1.42	0.882	0.504

dimension of the Cartesian space of the mobile manipulator is defined to be $r = 3$. At the initial point, the manipulator frame Σ_m is assumed to coincide with the world frame Σ_w. The starting joint position of the WMM is $q_0 = [0, 0, 0, 0, \pi/6, 0, \pi/2, 0, -\pi/6, 0]^{\mathrm{T}}$. Also, the starting position of the end-effector in Σ_w is $x_0 = [0.65, -0.0246, 0.4921]^{\mathrm{T}}$.

B. Experiment for End-effector Trajectory Tracking

To improve the tracking precision of the end-effector, the joint motion transferred to the mobile base ought to decrease if the joint limit of the manipulator is not reached. The traditional kinematic control and the proposed kinematic control (based on motion decomposition using a weighting matrix) are compared to verify the effectiveness of the latter. The traditional control method means using the pseudoinverse of the Jacobian J without adding a weighting matrix W_x defined in (12), expressed as $J^{\dagger} = J^{\mathrm{T}}(JJ^{\mathrm{T}})^{-1}$, to kinematically control the WMM [27]. If the desired end-effector trajectory is within the manipulator workspace, then the base will remain immobile with the proposed control approach. So, we define an end-effector trajectory beyond it, which is a circle with radius of 0.25 m, defined as $x_d(t) = x_0 + \big[-0.25(\cos(\pi/20t) - 1), -0.25\sin(\pi/20t), 0\big]^{\mathrm{T}}$. It is worth noting that the maximum radius of the circle within the manipulator workspace at this initial position is only 0.11 m. The control parameters are set as $K_x = 10I_{3\times3}$, $\epsilon = 0.2$, and the results of the experiment are shown in Figs. 5 and 6. It should be noted that the actual position of the end-effector is obtained via the motion capture system and the position of the mobile base is acquired by using the forward kinematics of the base. Table I contains the maximum and RMS values of the commanded base velocity in the experiment, where v_{xb}, v_{yb}, ω_b represent the commanded base velocities in x_b, y_b, and θ_b, respectively.

Table I shows that when the desired end-effector trajectory is beyond the manipulator workspace, the mobile base will be

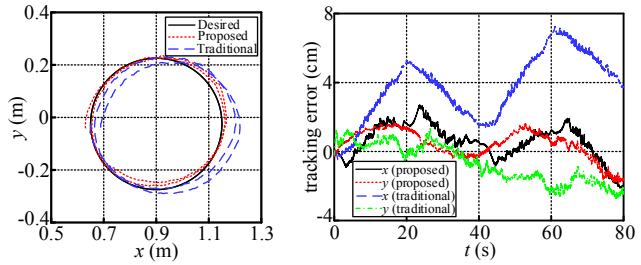

(a) End-effector trajectories (b) Tracking errors

Fig. 5: End-effector trajectory tracking beyond manipulator workspace.

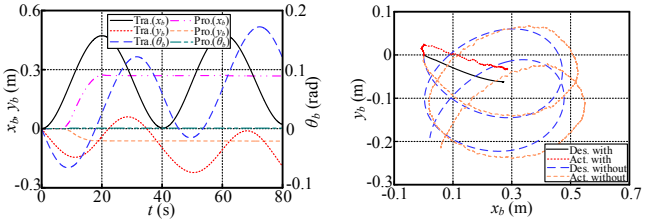

(a) Trajectories over time (b) Trajectories in x y plane

Fig. 6: Position of the mobile base during the experiment.

forced to move in both two scenarios. However, the velocity command to the base employing the proposed method is much smaller with the RMS value of velocity commands for x_b, y_b, and θ_b only representing 65.12%, 45.77%, and 6.94% of the commands via traditional method, respectively. Fig. 5 contains the end-effector tracking results. As shown in Fig. 5b, the maximum tracking error for x is reduced from 7.25 cm to 2.71 cm, and the maximum tracking error for y is decreased from 2.71 cm to 1.88 cm with motion distribution. Fig. 6 shows the position of the mobile base during the experiment with two different control methods. With the proposed approach, the mobile base moved only during time 7.15-20.35 s, while using the traditional approach, the mobile base was in motion ceaselessly (see Fig. 6a). Fig. 6b shows the desired and actual trajectories for the mobile base in the $x - y$ plane. The integral of the tracking error for the mobile base is defined as $\frac{\int_{T_s}^{T_f} |e_{i_b}| dt}{T}$, where T_s and T_f are the start time and final time for the motion of the base, T represents the total time for the experiment, and e_{i_b} represents the tracking error for the base in the two translational generalized coordinates. With the traditional method, the integral of the tracking errors in x_b and y_b were 3.79 cm and 1.09 cm, respectively, while these values were 0.53 cm and 0.49 cm with the proposed method. It is obvious that with the proposed method, the distributed motion to the base was much less, and the tracking accuracy was improved significantly.

C. Experiment for Force Exertion Capability Enhancement

The directional manipulability enhancement for manipulators can enhance the force exertion capability of the robotic system. The performance of the trajectory tracking method is verified in Section IV-B. Thus, this section will

focus on force exertion capability enhancement, however, motion decomposition is still adopted in the DM enhancement experiment to improve the tracking accuracy to the greatest extent. It should be noted that it is a trade-off between acquiring high tracking accuracy and achieving maximal force exertion capability since the former demands a motionless base and the latter requires a mobile base, and the proposed method tries its best to improve the tracking accuracy when force exertion capability is enhanced. It is noteworthy that when the minimum singular value of the Jacobian of the manipulator is below the predefined threshold for singularity avoidance, then, the damped least-squares method will be adopted. In our experiments, the minimum singular value did not become less than our predefined value (0.08), i.e., the WMM did not go very close to the singularity. Therefore, we did not employ the least-squares method during the experiments. The haptic interface is used by the user to provide the desired pushing movement for the end-effector, and it should be emphasized the proposed control methodology is for the entire WMM system with the specific motion decomposition decided by the weighting matrix in (12)-(14) automatically. The direction of the DM is defined as $u = J_I^{-1}[1,0,0]^{\mathrm{T}} \in \mathbb{R}^3$ to enhance the force exertion capability only along the x axis of the world frame, and J_I is a transformation matrix, defined in (20), that keeps u aligned with x of the world frame when the base is rotated. The other parameters for the experiment are set as $K_x = 10I_{3\times3}$, $\epsilon = 0.2$, $W_\tau = \mathrm{diag}(1,1,1,1,2.5,2.5,2.5)$, $k_C = 0.01$, and $k_H = 0.2$. The DM enhancement in Cartesian space is only conducted in the z direction, which is the height of the end-effector from the world frame, with the upper and lower limits defined as 0.56 m and 0.36 m, respectively, because the mobile base can move freely in the $x-y$ plane, the optimization on these two directions has difficulty in determining the position limit. It is worth mentioning that in the experiment, u is not constant since the mobile base may rotate; thus, the practicability of the proposed method in $x-y$ plane can be verified. And for its effectiveness in z direction (load carrying enhancement) of the world frame, a simulation has been conducted.

During the simulation, all the control parameters are set the same as in the experiment with the optimization direction defined as $u = [0,0,1]^{\mathrm{T}} \in \mathbb{R}^3$. The simulation results show that with the proposed approach, the DM can be enhanced from 1.125 to 4.031. If a z force of 10 N is applied to the end-effector, the norm of the weighted joint torque will decrease from 8.89 Nm to 2.48 Nm, which demonstrates the validity of the suggested method in enhancing the force exertion capability in z direction.

In the box pushing experiment, the box used is approximately 26 kg, and the goal is to push it about 0.2 m forward. The experimental results are shown as follows. Fig. 7 shows the configuration of the WMM with and without DM enhancement. It should be noted that the experiments were performed very slowly (i.e., quasi-static) to remove the effect of the inertia of the box. With the assumption that the friction force between the box and the ground was

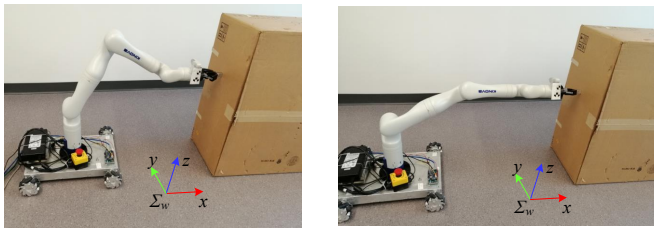

(a) Without DM enhancement (b) With DM enhancement

Fig. 7: Final configuration of the mobile manipulator during the task.

invariable, the WMM needs to apply the same force to the box so that the box would be moved (i.e., $F_{rob} > F_{fric}$, where F_{rob} is the pushing force by the robot, and F_{fric} is the friction force between the box and the ground). Fig. 7b shows that with the proposed method, the manipulator will go to a more desirable configuration to push the box. This is similar to how humans use their hands and body to push on a heavy object. However, with DM enhancement in x, the manipulator is almost fully stretched (cannot move much further in x), and most of the pushing motion will then be distributed to the base according to (11)-(14); thus, the trajectory tracking accuracy will inevitably be reduced.

It is worth mentioning that the DM enhancement is only desirable for the case in which the WMM requires large force capability (e.g., the push task). For the movement in the free space, it is beneficial to enhance the velocity manipulability ellipsoid (i.e., maximization of H_1). This will allow the user to have an agile mobile manipulator in the free space and a mobile manipulator with large force capability for the case of contact with the environment.

Fig. 8 shows the joint torque of the manipulator during the task. It should be noted that the joint torque is obtained via joint torque sensors, the gravity of the system has been subtracted, and the torque limits of the manipulator are 32 Nm for the first four joints and 13 Nm for the last three joints. The push task started at about 20 s, and without DM enhancement, the task could not be completed because joint four was saturated at time 23 s, as shown in Fig. 8a. However, as shown in Fig. 8b, with the proposed method, the task could be completed with the maximum joint torque no more than 20 Nm.

DM and the norm of the weighted joint torque during the experiment are shown in Fig. 9. Fig. 9a depicts the DM of the manipulator, with the proposed kinematic controller, the DM was first enhanced in Cartesian space from 3.825 to 3.905 during time 0-5 s, and the end-effector position in z was changed from 0.492 m to 0.456 m. Next, during time 5-20 s, the DM was enhanced using the null-space controller from 3.905 to 5.88, and then the push task started. Fig. 9b shows the norm of the weighted joint torque during the push process. The box was pushed about 0.25 m with the proposed method, and the norm of the weighted joint torque stayed at about 7.5 Nm; however, without adopting it, the norm increased rapidly to more than 10 Nm and stopped the task, which indicates the effectiveness of the proposed method.

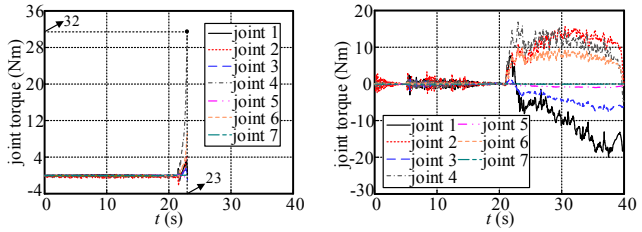

(a) Without DM enhancement (b) With DM enhancement

Fig. 8: Joint torque output of the manipulator during the experiment.

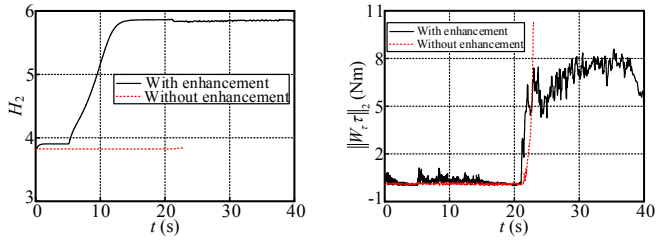

(a) Directional manipulability (b) Norm of weighted torque

Fig. 9: DM and norm of the weighted joint torque during the experiment.

V. Conclusions

A method to enhance the force exertion capability for a WMM and maintain high position tracking precision is proposed in this paper. The force exertion capability is improved by maximizing the directional manipulability in Cartesian space and the null-space of the system successively. Also, the end-effector trajectory error is minimized by transferring less of the desired total motion to the mobile base due to its low motion accuracy. The effectiveness of the proposed method has been experimentally verified by tracking a desired end-effector trajectory and pushing on a heavy box. During the trajectory tracking experiment, the maximum tracking error of the end-effector has been improved by 62.6% and 30.6% in x and y, respectively. In the box pushing experiment, with the proposed method, the massive box can be pushed with the norm of the weighted joint torque about 7.5 Nm, while without using it, the task cannot be executed with the norm going rapidly to more than 10 Nm. This method can enhance the force exertion capability in any desired direction. Our future work will focus on making a bilateral teleoperation system in which the WMM is haptically teleoperated from one or two user interfaces.

References

[1] D. Wahrmann *et al.*, "An autonomous and flexible robotic framework for logistics applications," *Journal of Intelligent & Robotic Systems*, vol. 93, no. 3-4, pp. 419–431, 2019.

[2] E. Dean-Leon *et al.*, "Tomm: Tactile omnidirectional mobile manipulator," in *2017 IEEE International Conference on Robotics and Automation (ICRA)*. IEEE, 2017, pp. 2441–2447.

[3] H. Zhang *et al.*, "Sensor-based redundancy resolution for a nonholonomic mobile manipulator," in *2012 IEEE/RSJ International Conference on Intelligent Robots and Systems*. IEEE, 2012, pp. 5327–5332.

[4] H. Seraji, "A unified approach to motion control of mobile manipulators," *The International Journal of Robotics Research*, vol. 17, no. 2, pp. 107–118, 1998.

[5] A. De Luca *et al.*, "Kinematic modeling and redundancy resolution for nonholonomic mobile manipulators," in *Proceedings 2006 IEEE International Conference on Robotics and Automation, 2006. ICRA 2006.* IEEE, 2006, pp. 1867–1873.

[6] A. De Luca *et al.*, "The reduced gradient method for solving redundancy in robot arms," *Robotersysteme*, vol. 7, no. 2, pp. 117–122, 1991.

[7] Y. Nakamura *et al.*, "Inverse Kinematic Solutions With Singularity Robustness for Robot Manipulator Control," *Journal of Dynamic Systems, Measurement, and Control*, vol. 108, no. 3, pp. 163–171, 1986.

[8] T. F. Chan *et al.*, "A weighted least-norm solution based scheme for avoiding joint limits for redundant joint manipulators," *IEEE Transactions on Robotics and Automation*, vol. 11, no. 2, pp. 286–292, 1995.

[9] B. Bayle *et al.*, "Manipulability of wheeled mobile manipulators: Application to motion generation," *The International Journal of Robotics Research*, vol. 22, no. 7-8, pp. 565–581, 2003.

[10] T. Yoshikawa, "Manipulability of robotic mechanisms," *The International Journal of Robotics Research*, vol. 4, no. 2, pp. 3–9, 1985.

[11] H. Xing *et al.*, "Unknown geometrical constraints estimation and trajectory planning for robotic door-opening task with visual teleoperation assists," *Assembly Automation*, vol. 39, no. 3, pp. 479–488, 2019.

[12] Y. Jia *et al.*, "Coordinated motion control of a nonholonomic mobile manipulator for accurate motion tracking," in *2014 IEEE/RSJ International Conference on Intelligent Robots and Systems*. IEEE, 2014, pp. 1635–1640.

[13] D. Xu *et al.*, "Trajectory tracking control of omnidirectional wheeled mobile manipulators: robust neural network-based sliding mode approach," *IEEE Transactions on Systems, Man, and Cybernetics, Part B (Cybernetics)*, vol. 39, no. 3, pp. 788–799, 2009.

[14] V. Andaluz *et al.*, "Adaptive unified motion control of mobile manipulators," *Control Engineering Practice*, vol. 20, no. 12, pp. 1337–1352, 2012.

[15] A. Torabi *et al.*, "Application of a redundant haptic interface in enhancing soft-tissue stiffness discrimination," *IEEE Robotics and Automation Letters*, vol. 4, no. 2, pp. 1037–1044, 2019.

[16] S. L. Chiu, "Task compatibility of manipulator postures," *The International Journal of Robotics Research*, vol. 7, no. 5, pp. 13–21, 1988.

[17] A. Ajoudani *et al.*, "Choosing poses for force and stiffness control," *IEEE Transactions on Robotics*, vol. 33, no. 6, pp. 1483–1490, 2017.

[18] L. Xiao *et al.*, "Design and analysis of ftznn applied to the real-time solution of a nonstationary lyapunov equation and tracking control of a wheeled mobile manipulator," *IEEE Transactions on Industrial Informatics*, vol. 14, no. 1, pp. 98–105, 2017.

[19] B. Navarro *et al.*, "A framework for intuitive collaboration with a mobile manipulator," in *2017 IEEE/RSJ International Conference on Intelligent Robots and Systems (IROS)*. IEEE, 2017, pp. 6293–6298.

[20] A. Torabi *et al.*, "Dynamic reconfiguration of redundant haptic interfaces for rendering soft and hard contacts." *IEEE Transactions on Haptics*, 2020.

[21] S. Chiaverini *et al.*, *Redundant Robots*. Cham: Springer International Publishing, 2016, pp. 221–242.

[22] W. Li *et al.*, "Haptic tele-driving of wheeled mobile robots under nonideal wheel rolling, kinematic control and communication time delay," *IEEE Transactions on Systems, Man, and Cybernetics: Systems*, vol. 50, no. 1, pp. 336–347, Jan 2020.

[23] S. R. Buss, "Introduction to inverse kinematics with jacobian transpose, pseudoinverse and damped least squares methods," *IEEE Journal of Robotics and Automation*, vol. 17, no. 16, pp. 1–19, 2004.

[24] S. Chiaverini, "Singularity-robust task-priority redundancy resolution for real-time kinematic control of robot manipulators," *IEEE Transactions on Robotics and Automation*, vol. 13, no. 3, pp. 398–410, 1997.

[25] F. Flacco *et al.*, "Control of redundant robots under hard joint constraints: Saturation in the null space," *IEEE Transactions on Robotics*, vol. 31, no. 3, pp. 637–654, 2015.

[26] F. Chen *et al.*, "Dexterous grasping by manipulability selection for mobile manipulator with visual guidance," *IEEE Transactions on Industrial Informatics*, vol. 15, no. 2, pp. 1202–1210, 2018.

[27] J. P. Puga *et al.*, "Optimal trajectory planning for a redundant mobile manipulator with non-holonomic constraints performing push–pull tasks," *Robotica*, vol. 26, no. 3, pp. 385–394, 2008.